



## Differential diagnostic value of $^{18}\text{F}$ -FDG PET/CT in osteolytic lesions

Xiaomeng Li, Ning Wu\*, Wenjie Zhang, Ying Liu, Yue Ming

Department of PET/CT, National Cancer Center/Cancer Hospital, Chinese Academy of Medical Sciences and Peking Union Medical College, Beijing, China

### ARTICLE INFO

#### Keywords:

PET/CT  
Fluorodeoxyglucose  
Bone  
Metastasis  
Multiple myeloma  
Osteolytic lesion

### ABSTRACT

**Background:** Both bone metastases and multiple myeloma (MM) are malignant diseases that can appear osteolytic on imaging and are difficult to differentiate. While positron emission tomography/computed tomography (PET/CT) has been demonstrated useful for the diagnosis of various bone lesions, correlations between PET/CT and histopathology and these diseases are unclear. This retrospective study investigated the optimal cutoff standardized uptake value (SUV) to differentiate MM and bone metastasis.

**Methods:** Patients with newly diagnosed osteolytic lesions ( $n = 344$ ) and suspected malignancy underwent both fluorodeoxyglucose (FDG) PET/CT and biopsy/surgery. FDG uptake and morphologic changes (e.g., soft tissue mass formation) were compared with pathological results.

**Results:** A total of 8896 osteolytic lesions were evaluated. The SUVmax of MM osteolytic lesions ( $1.6 \pm 0.7$ ) was significantly lower than that of bone metastases ( $5.5 \pm 2.7$ ;  $p = 0.000$ ). The best cutoff SUVmax for differentiating MM and bone metastasis was 2.65 (sensitivity 86.1%, specificity 94.7%;  $p = 0.000$ ). The SUVmax of bone lesions of soft tissue mass was higher than that for pure osteolytic lesions ( $p = 0.000$ ). A greater percentage of patients with bone metastasis had a soft tissue mass (7%) than did patients with MM (2%). The mean SUVmax of bone metastases was  $5.5 \pm 2.7$  (0.4–30.4); that of primary tumors was  $7.5 \pm 4.2$  (1.0–28.5). The SUVmax of bone metastases significantly correlated with the SUVmax of primary tumors ( $r = 0.532$ ;  $p = 0.000$ ).

**Conclusions:** FDG PET/CT is a valuable tool to differentiate osteolytic lesions. The best cutoff value of SUVmax for differentiating MM from bone metastasis is 2.65. The significant correlation between the SUVmax of bone metastasis and that of primary tumors is helpful for detecting primary tumors.

### 1. Introduction

Patients with bone destruction are often encountered in clinical practice. Bone destruction may be due to any of the following: bone metastases from an occult primary tumor, multiple myeloma (MM), lymphoma, sarcoma, primary bone tumors, bone tuberculosis, or osteomyelitis. The diagnosis of bone metastasis is facilitated when a primary tumor is obvious on positron emission tomography/computed tomography (PET/CT). However, if there is no primary tumor a diagnosis may be difficult.

Bone metastases and MM are both examples of malignant osseous diseases. Bone metastases occur in up to 70% of patients with advanced breast or prostate cancer, and in ~15–30% of patients with lung, stomach, colon, rectum, thyroid, or kidney cancer [1]. For the oncologist, the presence of bone metastases will suggest a major change in therapeutic approach.

MM accounts for ~1% of all malignancies and ~10% of hematologic neoplasms. MM may consist of diffuse marrow infiltration, focal bone lesions, or soft-tissue disease [2], and an accurate assessment of bone lesions is very important for directing therapy [3].

The usefulness of PET/CT for diagnosing various bone lesions has been demonstrated [4–12]. The accumulation rate of 18-fluoro-2-deoxy-D-glucose ( $^{18}\text{F}$ -FDG) in PET/CT, measured as the standardized uptake value (SUV), reflects the metabolic status of tumors. Determining the maximum SUV (SUVmax) facilitates a diagnosis, and areas of SUVmax are considered high-yield sites for biopsies. While diagnosis via histopathology remains the gold standard, correlations between histopathology and PET/CT characteristics with regard to bone metastases and MM have not been definitively elucidated. In China, the previous relevant studies were limited by small or moderate sample size, or investigations of a correlation between bone metastases and primary tumors were not conducted [13,14].

**Abbreviations:** DKK1, Dickkopf-related protein 1; FDG, fluorodeoxyglucose; MM, multiple myeloma; PET/CT, positron emission tomography/computed tomography; RANK, receptor activator of nuclear factor kappa-B; SUV, standardized uptake value; VEGF, vascular endothelial growth factor

\* Corresponding author at: Department of PET/CT, National Cancer Center/Cancer Hospital, Chinese Academy of Medical Sciences and Peking Union Medical College, Beijing 100021, China.

E-mail address: [cjr.wuning@vip.163.com](mailto:cjr.wuning@vip.163.com) (N. Wu).

<https://doi.org/10.1016/j.jbo.2020.100302>

Received 9 February 2020; Received in revised form 30 May 2020; Accepted 1 June 2020

Available online 13 July 2020

2212-1374/© 2020 Published by Elsevier GmbH. This is an open access article under the CC BY-NC-ND license (<http://creativecommons.org/licenses/by-nc-nd/4.0/>).

The objectives of this study were to determine the best cutoff value of SUV<sub>max</sub> for differentiating multiple myeloma and bone metastasis, and to investigate an association between the SUV<sub>max</sub> of bone metastases and that of primary tumors, which could be helpful in diagnosis. We retrospectively collected data from a large number of patients, treated at the largest cancer hospital in China. We retrospectively assessed the morphologic and metabolic findings of <sup>18</sup>F-FDG PET/CT in patients with osteolytic lesions, and compared these data with their pathological results.

## 2. Methods

### 2.1. Patients

A retrospective search of our institutional 18F-FDG PET/CT database revealed 344 patients (219 men and 125 women; mean age 58 y, age range 17–86 y) who had received a diagnosis between September 2009 and December 2015 of lytic bone lesions by imaging modalities such as X-ray, CT, or MRI. All these patients had undergone surgery or biopsy, and had pathology confirmed the diagnosis. The diseases of these patients included the following: miscellaneous cancers of the lung, breast, liver, gastrointestinal, esophagus, kidney, ureter, bladder, prostate, uterus, cervix; pancreas, gallbladder, thyroid, oral cavity, skin, neuroendocrine system, or thymus; sarcoma; malignancy of the lymphohematopoietic system such as MM, lymphoma, and leukemia; and others including angioendothelioma, chordoma, and benign lesions. Among them, there were 262 patients with bone metastasis (173 men, 89 women; mean age 57 y, age range 17–86 y) and 62 patients with MM (36 men, 26 women; mean age 59 y, age range 30–86 y) of MM.

### 2.2. Inclusion criteria

All lytic bone lesions, with or without soft tissue mass, were included in this study. Sclerotic or mixed bone lesions, or lesions with high 18F-FDG uptake but without obvious bone destruction on CT, were excluded from this study. In particular, lesions corresponding to osteoarthritis, benign joint disease, or traumas were carefully excluded from the analysis.

### 2.3. 18F-FDG PET/CT scans

All 18F-FDG PET/CT scans were performed in accordance with the standard protocol. Patients fasted  $\geq 6$  h and their pre-injection blood glucose levels were  $< 120$  mg/dL. Sixty to seventy minutes after the injection of 18F-FDG (dose 0.12–0.14 mCi/kg), imaging was started on a Discovery ST PET/CT scanner (General Electric Medical Systems, USA). The scan ranged from the top of the head to the upper femur level. If there were clinical indications of lower extremity bone lesions, the scan ranged from the top of the head to the bottom of the feet. The CT scan was first performed during quiet respiration using the following parameters: 120 kV, 150 mA, a pitch of 1.75, and 0.8 s tube rotation time. Subsequently, PET images were acquired in 3D mode (6–7 bed positions, 2.5 min/position for body and 2 bed positions, and 3 min/position for the head). The acquired data were reconstructed using an iterative reconstruction with CT-based attenuation correction.

### 2.4. Image analysis

Transaxial, sagittal, and coronal images and co-registered images were examined using Xeleris software (GE Healthcare). All 18F-FDG PET/CT images were visually evaluated and quantified by two radiologists. In the quantification of 18F-FDG uptake of lesions, SUV<sub>max</sub> was used. SUV<sub>max</sub> was calculated as the tissue concentration (mCi/kg) per injected dose (mCi) per body weight (kg).

### 2.5. Statistical analysis

Statistical analyses were performed using SPSS software V.17.0 (IBM SPSS). All statistical description data are expressed as mean  $\pm$  standard deviation (SD). Comparisons of mean values between groups were analyzed by the Mann-Whitney *U* test. Receiver-operating-characteristic (ROC) curve analysis was performed to estimate the best cutoff value of SUV<sub>max</sub> for the differentiation of bone metastasis and MM. Spearman's correlation test was performed to investigate an association between bone metastases and primary tumors.  $p < 0.05$  was considered statistically significant.

## 3. Results

A total of 8896 osteolytic lesions were identified on 18F-FDG PET/CT. Among them, there were 5492 lesions of MM and 3190 lesions of bone metastasis. The mean SUV<sub>max</sub> of MM ( $1.6 \pm 0.7$ ; range, 0.3–22.1) was significantly less than that for bone metastasis ( $5.5 \pm 2.7$ ; range, 0.4–30.4; ( $p = 0.000$ ).

We recorded the respective SUV<sub>max</sub> values of bone lesions with soft tissue mass formation and pure osteolytic lesions. Formation of soft tissue mass was found in 2% of MM patients, and 7% those with bone metastasis (Figs. 1 and 2, respectively). The mean SUV<sub>max</sub> of lesions with soft tissue mass formation in MM patients ( $5.6 \pm 3.4$ ) and bone metastasis patients ( $9.1 \pm 4.7$ ) was significantly higher than the mean SUV<sub>max</sub> of pure osteolytic lesions ( $1.2 \pm 0.9$  and  $5.2 \pm 2.8$ , respectively; all  $p = 0.000$ ; Table 1).

The SUV<sub>max</sub> values of osteolytic lesions were also significantly different between MM and each of various histologic cancer types or other malignant diseases (all  $p = 0.000$ ; Fig. 3). Among the malignant diseases, the SUV<sub>max</sub> of osteolytic lesions was lowest in MM ( $1.6 \pm 0.7$ ).

In ROC curve analysis the best cutoff value of SUV<sub>max</sub> in the differentiation of MM and bone metastasis was 2.65. The diagnostic sensitivity and specificity were 86.1% and 94.7%, respectively. The area under the ROC curve (AUC) was 0.942 ( $p = 0.000$ ).

In patients with bone metastases, the osteolytic lesion with the highest SUV<sub>max</sub> was used for the analysis (Table 2). The mean SUV<sub>max</sub> of bone metastases was  $5.5 \pm 2.7$  (range, 0.4–30.4), and the mean SUV<sub>max</sub> of primary tumors was  $7.5 \pm 4.2$  (range, 1.0–28.5). The SUV<sub>max</sub> of bone metastases significantly correlated with the SUV<sub>max</sub> of primary tumors ( $r = 0.532$ ;  $p = 0.000$ ).

## 4. Discussion

Bone metastases and MM are both malignant diseases. On medical imaging, both appear osteolytic, and therefore they are difficult to differentiate. In the present study, 262 of 344 patients (76.2%) were found to have bone metastases, diagnoses that were facilitated by the evidence of primary lesions. However, the remaining patients (23.8%) lacked an obvious primary lesion. We compared the results of PET/CT with the pathological diagnosis, and determined the best cutoff value of SUV<sub>max</sub> to differentiate MM and bone metastasis. We also found a significant positive correlation between the SUV<sub>max</sub> of bone metastases and the SUV<sub>max</sub> of primary tumors. This can be helpful for the identification of primary lesions in clinical work.

This study showed that the mean SUV<sub>max</sub> of MM osteolytic lesions ( $1.6 \pm 0.7$ ) is significantly lower than that of bone metastases ( $5.5 \pm 2.7$ ;  $p = 0.000$ ). Similar findings have been reported by other authors. Dai et al.'s [13] report concerned 26 patients with MM and 20 with bone metastasis. The SUV<sub>max</sub> of MM ( $3.4 \pm 2.0$ ) was significantly lower than that of bone metastases ( $p < 0.05$ ). Li et al. [14] retrospectively analyzed 21 patients with MM and 41 with bone metastasis and determined respective SUV<sub>max</sub> values of  $3.4 \pm 2.0$  and  $8.0 \pm 4.9$  ( $p < 0.05$ ). In the present study, the best cutoff value of SUV<sub>max</sub> for differentiating MM and bone metastasis was 2.65

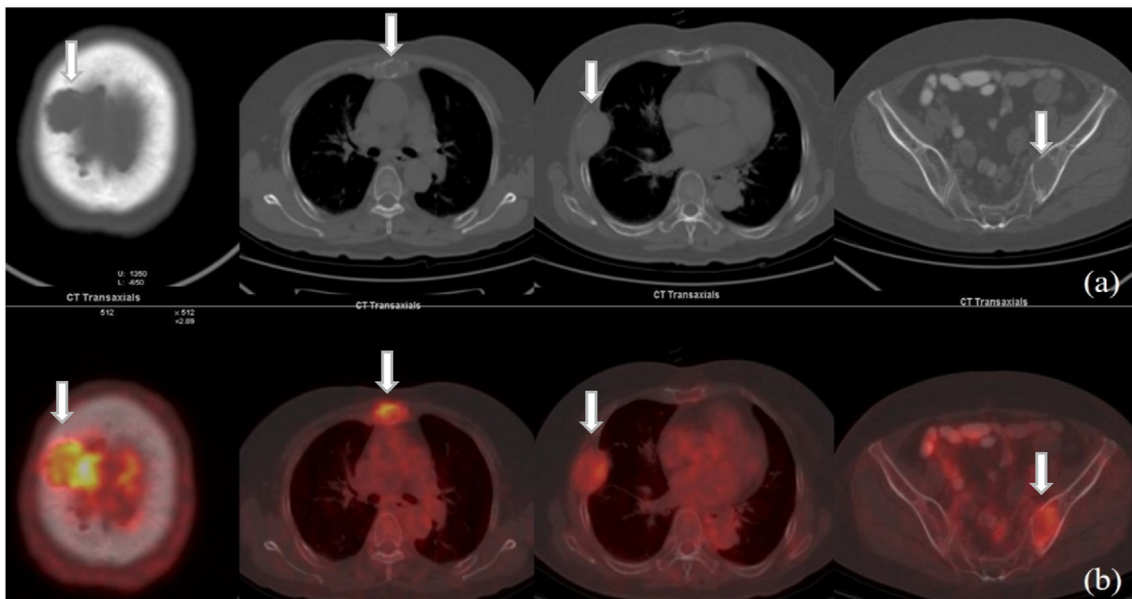


**Fig. 1.** A 76-year-old woman with MM. Multiple osteolytic lesions with increased uptake of  $^{18}\text{F}$ -FDG are shown on (a) transaxial CT, and (b) fused PET/CT. Parietal bone lesion had the highest  $\text{SUV}_{\text{max}}$ , of 5.1.  $\text{SUV}_{\text{max}}$  of the other lesions ranged from 1.0 to 3.1. Soft tissue mass was found in some osteolytic lesions.

(sensitivity 86.1% and specificity 94.7%;  $p = 0.000$ ). This is lower than the differential value of 4.45 reported by Dai et al. [13] (sensitivity 80.4% and specificity 72.4%;  $p < 0.05$ ). The difference in differential value may be due to selection bias related to sample size, as Dai et al.'s sample size was only 46 patients, while our population comprised 344 patients, among whom were 262 patients with bone metastases and 62 with MM. Unfortunately, Dai didn't mention the standard deviation range in his paper.

We used  $\text{SUV}_{\text{max}}$  as the main research parameter in our study because it is not affected by ROI, and it is the most commonly used parameter in our clinical work. There are other parameters as well, such

as  $\text{SUV}_{\text{mean}}$ ,  $\text{SUV}_{\text{peak}}$ . We have randomly selected 500 bone lesions (250 in MM, and 250 in metastases) and measured their  $\text{SUV}_{\text{max}}$ ,  $\text{SUV}_{\text{mean}}$  and  $\text{SUV}_{\text{peak}}$  (average SUV in  $1\text{ cm}^3$  volume sphere centered around the hottest pixel) in each lesion. The results were  $\text{SUV}_{\text{max}}$ :  $2.3 \pm 1.1$  vs.  $4.0 \pm 2.1$ ,  $P = 0.017$ ;  $\text{SUV}_{\text{mean}}$ :  $1.6 \pm 0.9$  vs.  $2.4 \pm 1.5$ ,  $P = 0.013$ ;  $\text{SUV}_{\text{peak}}$ :  $1.9 \pm 1.0$  vs.  $2.7 \pm 1.2$ ,  $P = 0.015$ . The  $\text{SUV}_{\text{mean/peak}}$  of MM was still significantly lower than that of bone metastases. We need to further study these parameters and the relationship between them and ROI.

The severity of malignant diseases can affect  $^{18}\text{F}$ -FDG uptake [8,15,16]. In general, only active lesions will show FDG uptake. MM

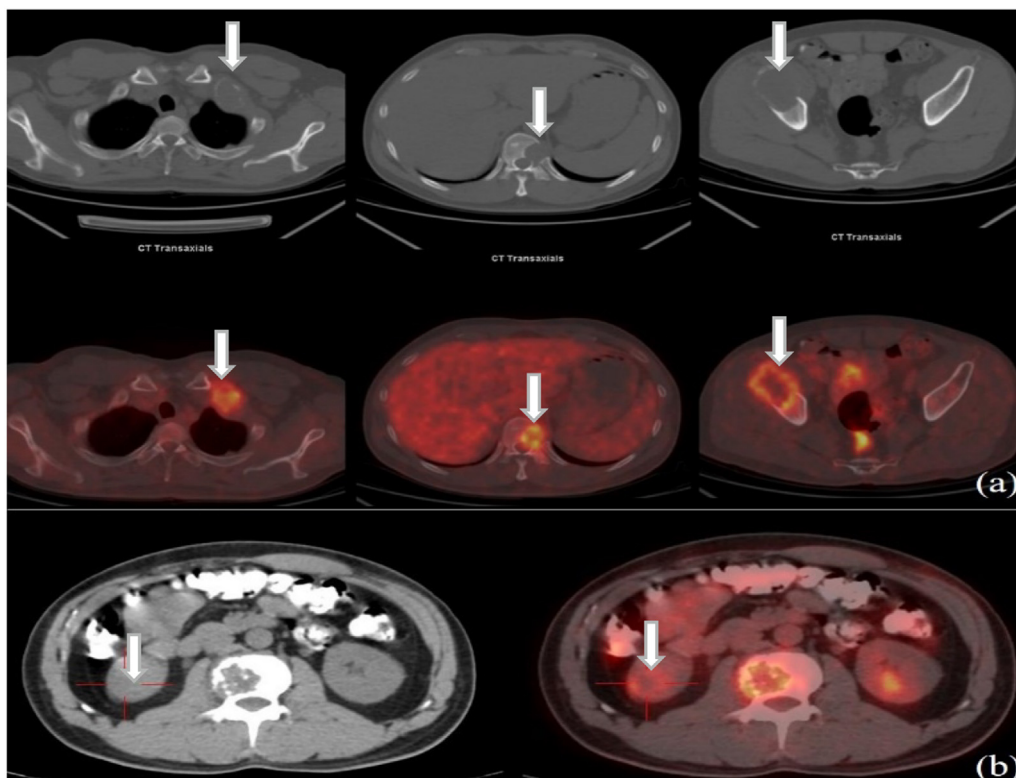


**Fig. 2.** Transaxial CT and fused PET/CT images of 43-year-old man with kidney cancer. (a) Multiple osteolytic metastases with increased uptake of  $^{18}\text{F}$ -FDG (the highest  $\text{SUV}_{\text{max}}$  7.3). (b) Of the Primary kidney cancer (red cross) showed increased uptake of  $^{18}\text{F}$ -FDG ( $\text{SUV}_{\text{max}}$  4.3). (For interpretation of the references to colour in this figure legend, the reader is referred to the web version of this article.)

**Table 1**  
Patient characteristics and SUVmax of each disease category.\*

	Patients, n	Lesions, n	Lytic		Mass	
			n (%)	SUVmax	n (%)	SUVmax
MM	62	5492	5393 (98%)	1.2 ± 0.9 (0.3–7.8)	99 (2%)	5.6 ± 3.4 (1.6–22.1)
Bone metastases	262	3190	2955 (93%)	5.2 ± 2.8 (0.4–24.4)	235 (7%)	9.1 ± 4.7 (2.1–30.4)
Lung cancer	148	1456	1326 (91%)	5.8 ± 2.6 (0.7–18.7)	130 (9%)	8.9 ± 4.1 (3.0–27.2)
Gastric cancer	10	482	478 (99%)	5.2 ± 3.2 (0.9–23.8)	4 (1%)	10.8 ± 2.7 (8.5–14.1)
Liver cancer	7	274	266 (97%)	2.6 ± 1.9 (0.4–9.0)	8 (3%)	3.8 ± 2.1 (2.4–8.7)
Breast cancer	6	206	194 (94%)	6.1 ± 2.9 (1.9–20.0)	12 (6%)	10.7 ± 3.9 (5.5–17.1)
Neuroendocrine cancer	7	115	110 (96%)	5.0 ± 1.9 (1.211.6)	5 (4%)	13.4 ± 9.7 (5.9–30.4)
Prostatic cancer	5	93	89 (96%)	4.7 ± 1.5 (0.8–9.7)	4 (4%)	10.2 ± 5.8 (6.2–18.8)
Kidney cancer	12	85	70 (82%)	5.6 ± 2.1 (2.6–14.3)	15 (18%)	7.9 ± 4.6 (2.9–21.1)
Skin cancer	6	85	85 (100%)	4.1 ± 1.8 (0.8–9.1)	0	0
Esophagus cancer	2	59	59 (100%)	5.0 ± 1.8 (2.0–11.6)	0	0
Oral cavity cancer	3	44	44 (100%)	6.8 ± 5.5 (2.0–24.4)	0	0
Cervical cancer	5	36	36 (100%)	4.8 ± 1.7 (2.69.4)	0	0
Uterine cancer	2	19	14 (74%)	6.6 ± 2.3 (4.1–10.7)	5 (26%)	8.8 ± 0.7 (7.8–9.7)
Thyroid cancer	2	16	8 (50%)	5.1 ± 1.1 (3.8–6.7)	8 (50%)	6.4 ± 4.3 (3.8–17.0)
Pancreatic cancer	3	15	12 (80%)	6.7 ± 2.0 (3.2–9.1)	3 (20%)	8.3 ± 1.9 (6.5–10.2)
Thymic cancer	3	10	9 (90%)	4.6 ± 2.0 (2.4–8.1)	1 (10%)	10.7 (NA)
Lymphoma	15	72	53 (74%)	6.8 ± 2.8 (2.0–17.6)	19 (26%)	12.0 ± 7.6 (2.1–28.5)
Leukemia	2	40	40 (100%)	3.0 ± 0.9 (1.2–5.9)	0	0
Sarcoma	11	46	32 (70%)	6.9 ± 2.6 (2.1–12.0)	14 (30%)	8.6 ± 3.4 (2.4–16.4)

\*Some results are not shown due to the small number of cases. NA, not applicable.

has a rather low metabolic activity [17,18], and in MM a high uptake of 18F-FDG by tumor cells is associated with the metabolic activity of the tumor [15]. When solid myeloma nodules are formed, they can be detected on PET scans [19]. In our study, the SUVmax of MM (1.6 ± 0.7) was significantly lower than that of any histologic subtype of cancer or other malignant disease, including sarcoma and lymphoma (p = 0.000).

PET with 18F-FDG detects tumors according to glucose demand, the

local cell density, and the metabolic activity of the surrounding tissue. The uptake of FDG is influenced by the tumor type, as well as differences in blood supply and tumor hypoxia, which further increase FDG uptake [3]. Unlike bone metastases from most other solid primary tumors, MM has a rather low metabolic activity, because the local cell density is low. MM releases the RANK (receptor activator of nuclear factor kappa-B) ligand, stimulating osteoclasts and Dickkopf-related protein 1 (DKK1). The latter is a protein that inhibits osteoblastic

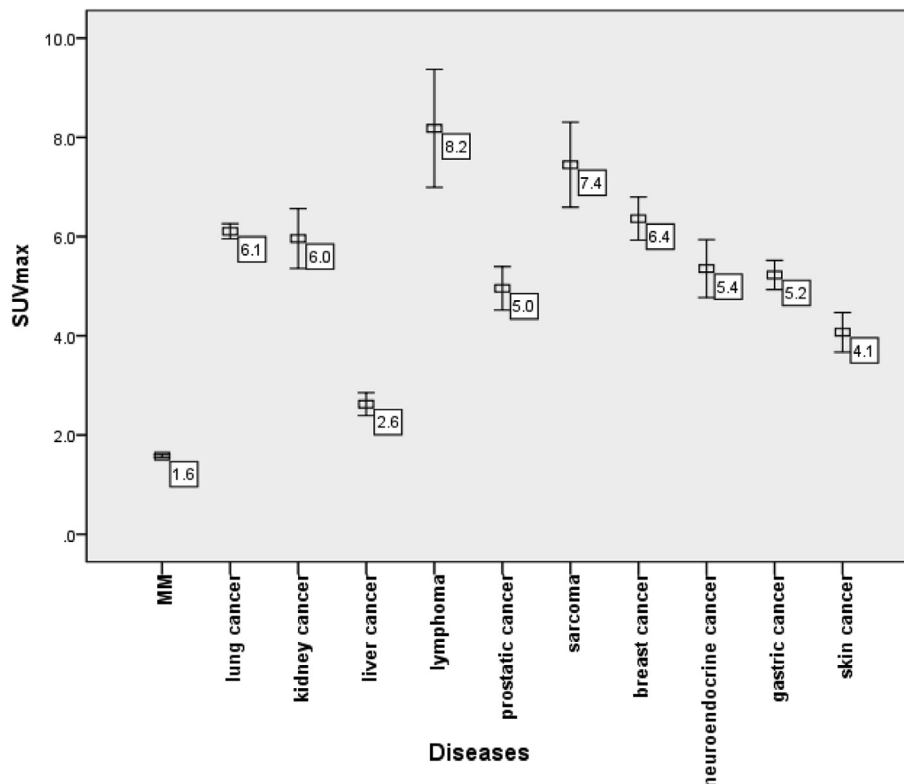


**Fig. 3.** SUV<sub>max</sub> of osteolytic lesions in each disease. Among these, MM had the lowest SUV<sub>max</sub> (1.6 ± 0.7). The SUV<sub>max</sub> of MM was significantly lower than that of any other malignant disease (all p = 0.000).

**Table 2**  
SUVmax of each cancer.\*

	Primary tumors	Bone metastases
Lung	7.8 ± 3.6	6.1 ± 2.9
Liver	5.4 ± 3.8	2.6 ± 1.9
Kidney	7.7 ± 5.3	6.0 ± 2.8
Gastric	5.6 ± 5.3	5.2 ± 3.2
Prostatic	5.3 ± 2.5	5.0 ± 2.1
Breast	5.0 ± 4.9	6.4 ± 3.1
Neuroendocrine	6.1 ± 2.4	5.4 ± 3.1
Skin	6.7 ± 3.1	4.1 ± 1.8

\*Some results are not shown due to the small number of cases.

function and results in lytic bone lesions. MM lesions are hardly detected on PET when only diffuse bone marrow involvement is present [19]. One study showed that, compared to patients with secretory MM, oligo/non-secretory MM patients had less extensive bone marrow infiltration [20]. Another study indicated that, there was a significant correlation between SUVmax values and bone marrow biopsy cellularity and plasma cell ratios ( $r = 0.54$  and  $r = 0.74$ ,  $p < 0.01$ ) [21]. We speculated that secretory MM might have a higher SUV than oligo/non-secretory MM. Thus, the SUV<sub>cutoff</sub> still relevant for all MM patients regardless of secretory status of MM cells. Unfortunately, in our study, all the MM patients were secretory MM. We need to further expand the sample size and include other oligo/non-secretory MM patients to verify this hypothesis.

The present study also found that the mean SUVmax of bone lesions with soft tissue mass formation ( $5.6 \pm 3.4$ ) was significantly higher than the SUVmax of pure osteolytic lesions ( $1.2 \pm 0.9$ ) in MM, and also in bone metastases ( $9.1 \pm 4.7$  cf.  $5.2 \pm 2.8$ ; both  $p = 0.000$ ). In addition, the mean SUV of each of the pathologies (cancer or other malignant disease including MM) were, respectively, significantly higher than the SUV of pure osteolytic lesions (all  $p = 0.000$ ). The reason for greater avidity for 18F-FDG uptake in osteolytic metastases with soft tissue mass is unknown, but may reflect a higher glycolytic rate in this type of metastasis [4,19]. Adams et al. [1] found that cortical destruction and surrounding soft tissue mass in bone lesions usually indicated a high degree of malignancy.

We found that the formation of soft tissue mass was more common in bone metastases (7%) than in MM (2%). The percentage of patients with soft tissue mass was high in those with thyroid, uterine, or kidney cancer (50%, 26%, and 18%, respectively), but lower in those with skin, gastric, or liver cancer (none, 1%, 3%). Mizumoto et al. [22] reported that in 603 patients with bone metastasis from lung, breast, gastrointestinal, prostate, and other cancers, 18.4% were observed with soft tissue formation. Chua et al. [16] noted that bone metastases of kidney cancer had a higher frequency of associated soft tissue masses than did most other cancers. In the present study, the frequency of bone metastases with soft tissue mass was high in kidney cancer, but lower in thyroid and uterine cancer.

Chen et al. [4] reported that hepatocellular carcinoma is susceptible to formation of soft tissue mass, more so than in other cancer types. However, the present study found that thyroid cancer was much more likely than hepatocellular carcinoma to form soft tissue mass: 50% of thyroid cancer patients developed soft tissue mass, whereas this was true of only 3% of hepatocellular carcinoma patients. Susceptibility to the formation of soft tissue mass in bone metastasis may depend on the type of primary cancer. For cancers with a rich blood supply, vascular endothelial growth factor (VEGF) is found in abundance and may facilitate the formation of a metastatic niche and subsequent mass. A previous study found that patients with bone metastasis had significantly higher levels of VEGF, compared with those without bone metastasis [23].

In the present study, in patients with bone metastases the mean SUVmax of bone metastases was  $5.5 \pm 2.7$ , ranging from 0.4 to 30.4,

while the mean SUVmax of primary tumors was  $7.5 \pm 4.2$ , ranging from 1.0 to 28.5. In most types of cancer (e.g., lung, liver, kidney, gastric, prostate, neuroendocrine, and skin), the SUVmax of the primary tumor was slightly higher than that of the bone metastases. In addition, the SUVmax of bone metastases positively correlated with the SUVmax of primary tumors ( $r = 0.532$ ;  $p = 0.000$ ). These results may aid detection of primary tumors in patients with metastatic bone cancer of unknown primary origin.

Nevertheless, in breast cancer, the result is just the opposite: the SUVmax of the primary tumor ( $5.0 \pm 4.9$ ) is slightly lower than that of bone metastases ( $6.4 \pm 3.1$ ). The cause of this is unclear. A possible explanation could be that the primary tumor has lower cellular density, proliferation rate, or number of glucose transporters compared with the metastasis. In addition, the pathological subtype of the primary tumor may be related to this result. Dashevsky et al. [24] found that the FDG avidity of bone metastases, as measured by SUVmax, was lower in patients with invasive lobular cancer than in those with invasive ductal cancer, just as primary lobular breast cancers show lower FDG avidity than do primary ductal breast cancers.

The quality and statistical power of the present research was enhanced by the large number of patients, who all had undergone both 18F-FDG PET/CT and surgical biopsy, with the latter subjected to histopathological examination. Thus, conclusions regarding 18F-FDG PET/CT were verified by reference to the pathology report. We also were able to evaluate various histologic subtypes of malignant diseases, including miscellaneous cancers (lung, breast, liver, gastrointestinal, kidney; prostatic, skin, neuroendocrine), sarcoma, and malignancy of the lymphohematopoietic system (MM, lymphoma). To obtain a complete evaluation, we analyzed in each patient not only the osteolytic lesion with the highest SUVmax, but all the osteolytic lesions. Finally, we studied both pure osteolytic lesions and lesions with soft tissue mass, and determined differences in FDG uptake.

There are, however, several shortcomings in our study. First, it was performed in the largest cancer hospital in China, so the results are only applicable to a similar (Asian) population, and no pediatric patients were included. Secondly, our results might entail a selection bias related to the retrospective nature of the data collection. Thirdly, not every bone lesion detected on PET/CT had histologic proof, as obtaining histologic proof of all bone lesions is impractical and unethical, and would not affect clinical management. Fourthly, the number of cases of some specific types of cancers was very small, and further large and multicentric prospective studies are needed to validate our findings. Finally, 18F-FDG may be less sensitive in detecting metastases from tumors with low FDG avidity, such as carcinoid tumors or some thyroid cancers [16]. Novel tracers may be introduced in the future that will overcome the deficiencies of FDG [25–29].

## 5. Conclusions

Images obtained by 18F-FDG PET/CT can provide both morphologic and metabolic findings, and hence are a valuable tool in the differential diagnosis of osteolytic lesions. Osteolytic lesions with a low SUVmax and no obvious primary lesion often suggest MM. The best cutoff value of SUVmax in the differentiation of MM and bone metastasis is 2.65. For patients with metastatic bone cancer of unknown primary origin, the positive correlation between the SUVmax of bone metastases and the SUVmax of primary tumors is helpful for the detection of primary tumors.

## CRedit authorship contribution statement

**Xiaomeng Li:** Conceptualization, Methodology, Software, Data curation, Writing - original draft. **Ning Wu:** Supervision. **Wenjie Zhang:** Investigation. **Ying Liu:** Methodology. **Yue Ming:** Software.

## Acknowledgements

We are very grateful to Dr. Xiuli Tao for help with statistical analyses.

## Funding

This project was financially supported by the Union Youth Science & Research Fund (No. 3332015061).

## Availability of data and material

All data generated or analyzed during this study are included in this published article. Further details are available upon request.

## Authors' contributions

XM L designed and performed the experiments and wrote the manuscript. NW conducted the experiments and revised the manuscript. WJ Z, YL, and YM contributed to the experimental work and data analysis. All authors read and approved the final manuscript.

## Competing interests

The authors declare that they have no competing interests.

## Consent for publication

Not applicable.

## Ethical approval and consent to participate

This retrospective study was approved by the local ethics committee. All tests were performed as part of standard clinical care. No additional study-related tests were performed. All patients signed informed consent for the use of their data for clinical or research work.

## Author details

Department of PET/CT, National Cancer Center/Cancer Hospital, Chinese Academy of Medical Sciences and Peking Union Medical College, Beijing, 100021, China.

## Appendix A. Supplementary data

Supplementary data to this article can be found online at <https://doi.org/10.1016/j.jbo.2020.100302>.

## References

- [1] H.J. Adams, J.M. de Klerk, B.G. Heggelman, S.V. Dubois, T.C. Kwee, Malignancy rate of biopsied suspicious bone lesions identified on FDG PET/CT, *Eur. J. Nucl. Med. Mol. Imaging* 43 (7) (2016) 1231–1238.
- [2] R.C. Walker, T.L. Brown, L.B. Jones-Jackson, L. De Blanche, T. Bartel, Imaging of multiple myeloma and related plasma cell dyscrasias, *J. Nucl. Med.* 53 (7) (2012) 1091–1101.
- [3] I. Ak, M.C. Sivriköz, E. Entok, E. Vardareli, Discordant findings in patients with non-small-cell lung cancer: absolutely normal bone scans versus disseminated bone metastases on positron-emission tomography/computed tomography, *Eur. J. Cardiothorac. Surg.* 37 (4) (2010) 792–796.
- [4] H.Y. Chen, X.M. Ma, Y.R. Bai, Radiographic characteristics of bone metastases from hepatocellular carcinoma, *Wspolczesna Onkol* 16 (5) (2012) 424–431.
- [5] K. Uchida, H. Nakajima, T. Miyazaki, T. Tsuchida, T. Hirai, D. Sugita, et al., 18F-FDG PET/CT for diagnosis of osteosclerotic and osteolytic vertebral metastatic lesions: comparison with bone scintigraphy, *Asian Spine J.* 7 (2) (2013) 96–103.
- [6] K. Glazebrook, F.L. Guerra Bonilla, A. Johnson, S. Leng, A. Dispenzieri, Computed tomography assessment of bone lesions in patients with POEMS syndrome, *Eur. Radiol.* 25 (2) (2015) 497–504.
- [7] B.Z. Dashevsky, D.A. Goldman, M. Parsons, M. Gönen, A.D. Corben, M.S. Jochelson, et al., Appearance of untreated bone metastases from breast cancer on FDG PET/CT: importance of histologic subtype, *Eur. J. Nucl. Med. Mol. Imaging* 42 (11) (2015) 1666–1673.
- [8] N.G. Schaefer, K. Strobel, C. Taverna, T.F. Hany, Bone involvement in patients with lymphoma: the role of FDG-PET/CT, *Eur. J. Nucl. Med. Mol. Imaging* 34 (1) (2007) 60–67.
- [9] P. Sharma, B.C. Khangembam, K.C. Suman, H. Singh, S. Rastogi, S.A. Khan, et al., Diagnostic accuracy of 18F-FDG PET/CT for detecting recurrence in patients with primary skeletal Ewing sarcoma, *Eur. J. Nucl. Med. Mol. Imaging* 40 (7) (2013) 1036–1043.
- [10] M.S. Virk, F.A. Petrigliano, N.Q. Liu, A.F. Chatziioannou, D. Stout, C.O. Kang, et al., Influence of simultaneous targeting of the bone morphogenetic protein pathway and RANK/RANKL axis in osteolytic prostate cancer lesion in bone, *Bone* 44 (1) (2009) 160–167.
- [11] H.S. Choi, Y. JeR, H.L. Park, E.K. Choi, S.H. Kim, W.H. Lee, Role of 18F-FDG PET/CT in differentiation of a benign lesion and metastasis on the ribs of cancer patients, *Clin. Imaging* 38 (2) (2014) 109–114.
- [12] V. Wenter, J.P. Müller, N.L. Albert, S. Lehner, W.P. Fendler, P. Bartenstein, et al., The diagnostic value of [18F]FDG PET for the detection of chronic osteomyelitis and implant-associated infection, *Eur. J. Nucl. Med. Mol. Imaging* 43 (4) (2016) 749–761.
- [13] D. Dai, W.G. Xu, Q. Wang, X.Y. Song, L. Zhu, J. Wang, et al., The value of SUV of FDG-PET/CT in differentiation of myeloma and metastasis in patients with malignant skeletal disease of unknown origin, *Chin. J. Orthop.* 29 (2009) 1127–1130.
- [14] X.J. Li, J.S. Zheng, J.M. Sun, N.N. Zhao, F.Q. Li, Diagnostic value of 18F-FDG PET/CT for differentiating multiple myeloma from bone metastases with undermined origin, *Chin. J. Nucl. Med. Mol. Imaging* 35 (2015) 284–288.
- [15] R. Haznedar, S.Z. Aki, O.U. Akdemir, Z.N. Ozkurt, O. Cemel, M. Yağcı, et al., Value of 18F-fluorodeoxyglucose uptake in positron emission tomography/ computed tomography in predicting survival in multiple myeloma, *Eur. J. Nucl. Med. Mol. Imaging* 38 (6) (2011) 1046–1053.
- [16] S. Chua, G. Gnanasegaran, G.J. Cook, Miscellaneous cancers (lung, thyroid, renal cancer, myeloma, and neuroendocrine tumors): role of SPECT and PET in imaging bone metastases, *Semin. Nucl. Med.* 39 (6) (2009) 416–430.
- [17] E. Mena, P. Choyke, E. Tan, O. Landgren, K. Kurdziel, Molecular imaging in myeloma precursor disease, *Semin. Hematol.* 48 (1) (2011) 22–31.
- [18] S. Sager, N. Ergül, H. Ciftci, G. Cetin, S.I. Güner, T.F. Cermik, The value of FDG PET/CT in the initial staging and bone marrow involvement of patients with multiple myeloma, *Skeletal Radiol.* 40 (2011) 843–847.
- [19] S. Delorme, A. Baur-Melnyk, Imaging in multiple myeloma, *Eur. J. Radiol.* 70 (3) (2009) 401–408.
- [20] M. Migkou, I. Avivi, M. Gavriatopoulou, Y.C. Cohen, D. Fotiou, et al., Clinical characteristics and outcomes of oligosecretory and non-secretory multiple myeloma, *Ann. Hematol.* 99 (6) (2020) 1251–1255.
- [21] Sait Sager, Nurhan Ergül, Hediye Ciftci, Güven Cetin, Sebnem Izmir Güner, et al., The value of FDG PET/CT in the initial staging and bone marrow involvement of patients with multiple myeloma, *Skeletal Radiol.* 40 (7) (2011) 843–847.
- [22] M. Mizumoto, H. Harada, H. Asakura, et al., Radiotherapy for patients with metastases to the spinal column: a review of 603 patients at Shizuoka Cancer Center Hospital, *Int. J. Radiat. Oncol. Biol. Phys.* 79 (2011) 208–213.
- [23] A.O. Kaseb, A. Hanbali, M. Cotant, M.M. Hassan, I. Wollner, P.A. Philip, Vascular endothelial growth factor in the management of hepatocellular carcinoma: a review of literature, *Cancer* 115 (2009) 4895–4906.
- [24] B.Z. Dashevsky, D.A. Goldman, M. Parsons, M. Gönen, A.D. Corben, M.S. Jochelson, et al., Appearance of untreated bone metastases from breast cancer on FDG PET/CT: importance of histologic subtype, *Eur. J. Nucl. Med. Mol. Imaging* 42 (2015) 1666–1673.
- [25] Masashi Kawaguchi, Ukihide Tateishi, Kazuya Shizukuishi, A. Suzuki, T. Inoue, 18F-fluoride uptake in bone metastasis: morphologic and metabolic analysis on integrated PET/CT, *Ann. Nucl. Med.* 24 (2010) 241–247.
- [26] C. Sachpekidis, H. Goldschmidt, D. Hose, L. Pan, C. Cheng, K. Kopka, et al., PET/CT studies of multiple myeloma using 18F-FDG and 18F-NaF: comparison of distribution patterns and tracers' pharmacokinetics, *Eur. J. Nucl. Med. Mol. Imaging* 41 (7) (2014) 1343–1353.
- [27] J.N. Talbot, F. Gutman, L. Fartoux, J.D. Grange, N. Ganne, K. Kerrou, et al., PET/CT in patients with hepatocellular carcinoma using [18F]fluorocholine: preliminary comparison with [18F]FDG PET/CT, *Eur. J. Nucl. Med. Mol. Imaging* 33 (11) (2006) 1285–1289.
- [28] Y. Nakamoto, K. Kurihara, M. Nishizawa, K. Yamashita, K. Nakatani, T. Kondo, et al., Clinical value of 11C-methionine PET/CT in patients with plasma cell malignancy: comparison with 18F-FDG PET/CT, *Eur. J. Nucl. Med. Mol. Imaging* 40 (5) (2013) 708–715.
- [29] M. Morita, T. Higuchi, A. Achmad, A. Tokue, Y. Arisaka, Y. Tsushima, Complementary roles of tumour specific PET tracer 18F-FAMT to 18F-FDG PET/CT for the assessment of bone metastasis, *Eur. J. Nucl. Med. Mol. Imaging* 40 (11) (2013) 1672–1681.